IAES International Journal of Robotics and Automation (IJRA)
Vol. 15, No. 1, March 2026, pp. 21~32
ISSN: 2722-2586, DOI: 10.11591/ijra.v15i1.pp21-32

Hybrid force/position approach for flexible-joint robot with fuzzy-super twisting sliding mode control

Rafik Amaini, Farid Ferguene
LRPE Laboratory, Automatic and Instrumentation Department, Université des Sciences et de la Technologie Houari Boumediene, Algiers, Algeria

Article Info

Article history:

Received May 27, 2025
Revised Nov 13, 2025
Accepted Dec 15, 2025

Keywords:

Fuzzy logic
High gain observer
Hybrid force/position control
Rigid-link flexible joint robot
Super-twisting sliding mode

ABSTRACT

This paper presents a novel hybrid force/position control strategy for rigid-link flexible-joint robots (RLFJR) operating in constrained environments. The proposed approach integrates fuzzy logic with the super-twisting sliding mode control (FSTSMC) algorithm to enhance robustness and reduce the chattering phenomenon typically associated with sliding mode controllers. A two-loop control structure is adopted: an inner loop dedicated to position control using the FSTSMC, and an outer loop for force regulation employing a classical PI controller. To address the challenge of limited joint state measurements in industrial robots, a high-gain nonlinear observer is designed for accurate joint state estimation. The effectiveness of the proposed method is validated through simulations on a PUMA 560 robot model, performing a circular trajectory while applying a constant contact force. Results demonstrate high tracking precision in both joint and Cartesian spaces, rapid convergence of errors, and significant mitigation of chattering effects, confirming the feasibility and efficiency of the proposed control scheme for interaction tasks involving flexible-joint manipulators.

Corresponding Author:

Rafik Amaini
LRPE Laboratory, Automatic and Instrumentation Department, Université des Sciences et de la Technologie Houari Boumediene
BP n°32 El Alia- Bab Ezzouar, 16111 Algiers, Algeria
Email: rafik.amaini@gmail.com

1. INTRODUCTION

The flexibility observed in industrial robot joints mainly results from the use of mechanical transmission elements such as belts, long connecting rods and harmonic drives. These components enhance the system's dynamic performance and allow for high reduction ratios. Nevertheless, when subjected to significant dynamic forces or load variations, they tend to display a certain inherent compliance [1].

Certain industrial robotic operations involve direct interaction with the environment, where the robot must generate and control relatively high contact forces. In such cases, joint flexibility can significantly affect task accuracy, potentially leading to instability. Therefore, it is essential to account for this phenomenon when modeling and designing force and position control systems [2].

A significant amount of research focuses on the control of rigid-link flexible-joint robots (RLFJR). Notably, control methods based on adaptive singular perturbation techniques and non-adaptive [3]–[6] have been developed. While effective for high joint stiffness, these techniques show limitations otherwise. Another approach is dynamic feedback linearization control [7]–[9], which requires the desired trajectory to be at least four times differentiable and joint acceleration measurements. Nonlinear PID and sliding mode control (SMC) are discussed in [10]–[13], respectively. In [14], the authors carried out a comparison between control

strategies based on singular perturbation theory and those relying on differential algebra formulations, while [15] compares proportional-integral controller (PI) and sliding mode controls.

Unlike rigid joints, flexible joints exhibit a discrepancy between the motor angle and the joint angle, doubling the number of state variables. Since most industrial robots only have motor position sensors, joint angle estimation requires a state observer. High-gain observers [16], sliding mode observers [17], and observer-based neural control [18] have been proposed for this purpose.

This work introduces a new control scheme for flexible joint robots performing tasks that involve environmental interaction. While numerous control schemes for RLFJR in free space have been proposed, fewer address tasks in constrained environments. In constrained environments, the same control approaches from free-space scenarios have been adapted, including singular perturbation control [19]–[21], dynamic feedback linearization control [22], [23], and neural-based control [24]. Sliding mode control is applied in [25] and [26].

Here, we propose a hybrid force/position control approach based on the fuzzy super-twisting sliding mode control (FSTSMC) technique for industrial flexible joint robots. Classical SMC has advanced significantly due to its robustness and finite-time convergence. However, the high-frequency switching causes "chattering", which can disturb or damage systems [27], [28].

To address this, higher-order sliding mode (HOSM) control was developed [27], mitigating chattering while maintaining classical SMC performance. HOSM control targets the derivatives of the sliding variable instead of the variable itself. When access to these derivatives is limited, the super-twisting sliding mode control [29] provides an alternative. Designed for systems with a sliding variable of relative degree one, this second-order controller eliminates the need for the sliding variable's second derivative. The super-twisting sliding mode control was analyzed geometrically through homogeneity in [30], while Lyapunov-based stability analysis is found in [31] and [32].

The main objective of this work is to develop a force-position control strategy for a rigid-link flexible-joint robot (RLFJR), taking into account joint flexibility, minimizing its adverse effects on task execution, and enhancing overall system efficiency. A novel hybrid control scheme is proposed for RLFJR operating in constrained environments, integrating the FSTSMC method, which combines fuzzy logic with the super-twisting algorithm to achieve accurate force and position tracking. This approach reduces the convergence time of tracking errors, improves robustness against external disturbances and parametric uncertainties, and effectively mitigates the joint flexibility effect. Furthermore, the integration of fuzzy logic helps suppress the chattering phenomenon commonly encountered in traditional sliding mode controllers.

2. PROPOSED CONTROLLER DESIGN

Our objective is to design a robust hybrid force/position control strategy that ensures the accuracy of (1) and (2), even under uncertainties and external disturbances.

$$\lim_{t\to t_f}\|e_q\| = \lim_{t\to t_f}\|(q - q_d)\| = 0 \tag{1}$$

$$\lim_{t\to t_f}\|e_F\| = \lim_{t\to t_f}\|(F - F_d)\| = 0 \tag{2}$$

Here, $q_d \epsilon R_n$ and $F_d \epsilon R_n$ represent the desired angular position and force, respectively. $e_q = (q - q_d)$ denotes the trajectory tracking error, $e_F = (F - F_d)$ represents the force error, and t_f is the finite time.

The hybrid force/position control scheme proposed in this study follows an implicit hybrid control approach, utilizing the external force feedback loop method introduced in [33] shown in Figure 1.

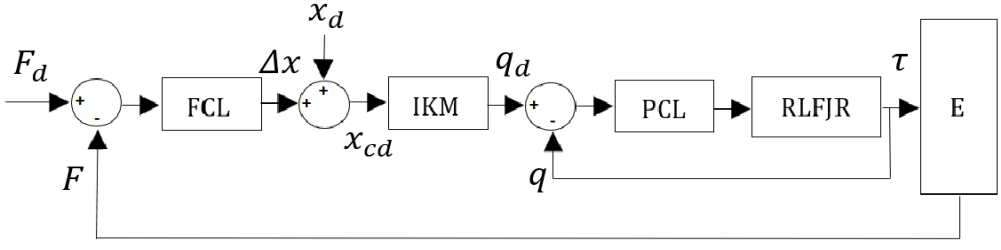

Figure 1. Structure of external force control loop

This hybrid force/position control scheme features a two-loop structure: an inner loop dedicated to position controller and an outer loop for force controller, implemented around the inner loop. This design is particularly advantageous for its simplicity in implementation, especially for industrial robots that often come equipped with an integrated position controller.

In this approach, the two control loops are designed independently. The output of the outer loop Δx is used to modify the desired trajectory x_d, generating a corrected desired trajectory x_{cd}. A proportional-integral controller (PI) governs the outer force control loop, while the inner position control loop is managed by a fuzzy super-twisting algorithm-based controller. Furthermore, an inverse kinematic model (*IKM*) is employed to accommodate the position controller's operation in joint space.

3. METHOD

This section presents the methodological framework adopted for the development of the proposed hybrid force-position control strategy applied to a rigid-link flexible-joint robot (RLFJR). The objective is to provide a detailed description of the modeling and control design process, highlighting each component of the controller architecture.

First, the dynamic model of the RLFJR is formulated to capture the effects of joint flexibility and to serve as a foundation for controller design. Then, a hierarchical control structure is developed, consisting of an outer loop for force regulation and an inner loop for position control. The position loop incorporates a state observer, a super-twisting sliding mode controller (STSMC), and a fuzzy logic-based adaptation mechanism to enhance robustness and reduce chattering.

Finally, the proposed control approach is applied to a PUMA 560 industrial robot to validate its performance through simulation. Each subsection provides the theoretical background, mathematical formulation, and control design steps required to implement the proposed strategy.

3.1. Dynamic modeling of the RLFJR

The dynamic model of a N-Regid link flexible joint robot (RLFJR) shown in Figure 2 is governed by (3) and (4),

$$M(q)\ddot{q} + C(q,\dot{q})\dot{q} + G(q) = \tau_e + J^T F \tag{3}$$

$$B\ddot{\theta} + \tau_e = \tau \tag{4}$$

where $q, \dot{q}, \ddot{q} \epsilon R_n$ and $\theta, \dot{\theta}, \ddot{\theta} \epsilon R_n$ denote the angular position, velocity, and acceleration of the links and motors, respectively. $M(q) \epsilon R_{n\times n}$ and $B \epsilon R_{n\times n}$ is the positive definite inertia matrix of the link and motor respectively, $C(q) \epsilon R_{n\times n}$ is the centripetal-Coriolis matrix, $G(q) \epsilon R_n$ is the gravitational of the link dynamics, $\tau \epsilon R_{n\times n}$ denotes the input torque vector, $F \epsilon R_m$ denote the vector of contact forces of the end-effector with the environment, $J(q) \epsilon R_{m\times n}$ is Jacobean matrix which relates the velocities of the joint and Cartesian spaces as (5),

$$\dot{x} = J(q)\dot{q} \tag{5}$$

where $x \in \mathbb{R}^m$represents the position vector of the end-effector. The environment is considered as a deformable and frictionless surface, where the contact force F is assumed to vary proportionally with the deformation of the environment.

$$F = K_e(x - x_e) \tag{6}$$

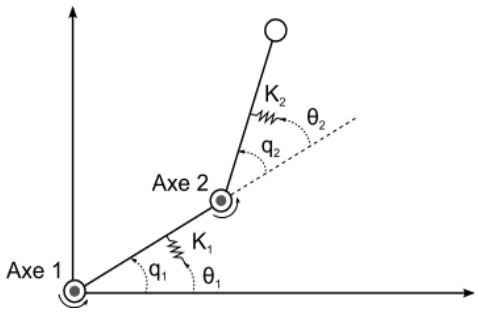

Figure 2. Robot with rigid bodies and flexible joints

Here $K_e \epsilon R_{m\times m}$ is the diagonal matrix of the environment stiffness, $x_e \epsilon R_m$ is the position of the environment at rest, $\tau \epsilon R_{n\times n}$ denotes the input torque vector, $\tau_e \epsilon R_n$ is the elastic torque at flexible joints and it is modeled by (7),

$$\tau_e = K(\theta - q) \tag{7}$$

where $K \epsilon R_{n\times n}$ is positive diagonal matrix of joints stiffness.

3.2. Force controller design

In the control scheme shown in Figure 1, a simple PI regulator shown in Figure 3 is utilized in the force control loop (FCL), where: $\Delta x = \frac{1}{K_e}\left(K_p e_F + K_i \int e_F\right)$. A proportional–integral (PI) controller contributes to improving transient behavior and eliminating static error. Yet, in such a control configuration, the proper design of the position controller remains essential for robustness against external perturbations.

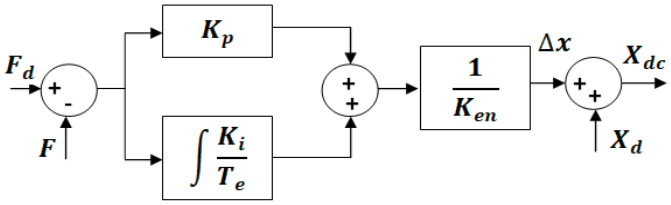

Figure 3. Structure of external force control loop

3.3. Position controller design

In this section, we will develop the inner loop for position control of the RLFJ robot, using the control scheme illustrated in Figure 4. As discussed earlier, the output of the force control loop is an increment, Δx, which is added to the desired trajectory to obtain a corrected desired trajectory, x_{cd}, in Cartesian space. This corrected trajectory must then be transformed into a joint space trajectory using the inverse kinematic model (IKM), expressed as $q_d = IKM(x_{cd})$.

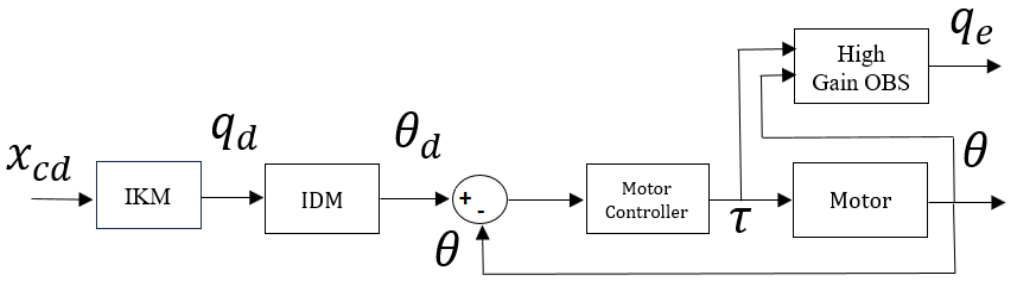

Figure 4. Position control loop

The position controller generates motor torque as its output. Unlike rigid robots, where the motor angle equals the joint angle $\theta = q$, the joint flexibility in this case means $\theta \neq q$. Therefore, the desired trajectory must be expressed in terms of motor angular position rather than joint position. To achieve this, the dynamic model of the RLFJ robot (3) is used to derive the inverse dynamic model (IDM).

$$M(q_d)\ddot{q_d} + C(q_d, \dot{q_d})\dot{q_d} + G(q_d) = K(\theta_d - q_d) + J^T F \tag{8}$$

$$\theta_d = \frac{1}{K}\left(M(q_d)\ddot{q_d} + C(q_d, \dot{q_d})\dot{q_d} + G(q_d)\right) - J^T F \tag{9}$$

One of the challenges in controlling an RLFJ robot is the incomplete information about the system's state. In industrial robots, typically assumed to be perfectly rigid, angular position sensors are installed on the

motors, providing joint position information based on the relationship $\theta = Nq$, where N is the transmission reduction ratio. For simplicity, we assume $N = 1$. However, in our case, the robot is not perfectly rigid $\theta \neq q$, meaning joint position cannot be directly measured from motor sensors. To address this, a high-gain observer will be implemented, which will be briefly discussed later. Furthermore, the motor controller block will employ the fuzzy super-twisting algorithm to generate the required motor torque.

3.3.1. High gain observer

Industrial robots are typically equipped with sensors that measure the angular positions θ and currents of their actuators. However, due to transmission flexibility, the robot's state cannot be directly measured from motor measurements. A common solution proposed in the literature is to use an observer to estimate the unmeasured states based on motor data.

In the robots considered here, the motor states (θ and $\dot{\theta}$) and the force are directly measured. However, the approach proposed in the next section requires knowledge of the robot body states (q and $\dot{q}$). To address this, the observer developed in this study is based on a nonlinear observer introduced in [16]. This observer estimates joint positions and body velocities using the measurements available from the motor axes.

Defining the state variables x, as $x_1 = q \quad x_2 = \dot{q}, \quad x_3 = \theta \quad x_4 = \dot{\theta}$ we obtain the following state space model.

$$\begin{aligned} \dot{x_1} &= x_2 \\ \dot{x_2} &= M(x_1)^{-1}[\tau_e + J^T F - C(x_1, x_2)x_2 - G(x_1)] \\ \dot{x_3} &= x_4 \\ \dot{x_4} &= B^{-1}[\tau - \tau_e] \end{aligned} \tag{10}$$

The output (measured) variables are $y_1 = x_3$ and $y_2 = x_4$. We propose the coordinate transformation in (11).

$$\begin{aligned} z_1 &= K^{-1}Bx_4 \\ z_2 &= x_1 \\ z_3 &= x_2 \end{aligned} \tag{11}$$

By differentiating the previous equations, we obtain (12).

$$\begin{aligned} \dot{z_1} &= z_2 - y_1 + K^{-1}\tau \\ \dot{z_2} &= x_2 \\ \dot{z_3} &= \Psi(z_2, z_3, y_1) \\ y_2 &= B^{-1}Kz_1 \end{aligned} \tag{12}$$

Here, $\Psi(z_2, z_3, y_1) = M^{-1}(z_2)[\tau_e + J^T F - C(z_2, z_3)z_3 - G(z_2)]$. The system (12) can be written as (13),

$$\begin{aligned} \dot{z} &= Az + g(z, y_1, u) \\ y_2 &= B^{-1}KCz \end{aligned} \tag{13}$$

with $A = \begin{bmatrix} 0 & I & 0 \\ 0 & 0 & I \\ 0 & 0 & 0 \end{bmatrix}$ et $C = [I \quad 0 \quad 0]$, when I and 0 are identity and zero matrices being of dimension $nxn.$, the vector g can be expressed as:

$$g(z, y_1, u) = \begin{bmatrix} K^{-1}u - y_1 \\ 0 \\ \Psi(z_2, z_3, y_1) \end{bmatrix}$$

We define the high-gain coefficient matrix as:

$$\Gamma = \begin{bmatrix} GI & 0 & 0 \\ 0 & G^2 I & 0 \\ 0 & 0 & G^3 I \end{bmatrix}$$

where $G \geq 1$ is a high-gain scalar constant. Select a matrix K_G such that all eigenvalues of $A - K_G C$ lie in the left half of the complex plane. Define the matrix $\bar{K}_G = K_G K^{-1} B$, and consider observer (14) corresponding to system (13).

$$\begin{aligned}\dot{\hat{z}} &= A\hat{z} + g(\overline{z}, y_1, u) + \Gamma\overline{K_G}(y_2 - B^{-1}KC\hat{z}) \\ \overline{z_3} &= \frac{\hat{z_3}}{\|\hat{z_3}\|} M_s \text{sat}\left(\frac{\|\hat{z_3}\|}{M_s}\right) \\ \overline{z_2} &= y_1 - \frac{y_1 - \hat{z_2}}{\|y_1 - \hat{z_2}\|} N_s \text{sat}\left(\frac{\|y_1 - \hat{z_2}\|}{N_s}\right)\end{aligned} \tag{14}$$

M_s and N_s are known positive physical constants, where $\|x_2\| < M_s$ and $\|x_1 - x_3\| < N_s$. The function $sat(\,)$ is defined as:

$$sat(x) = \begin{cases} x & \text{if} \quad |x| \leqslant 1 \\ 1 & \text{if} \quad |x| > 1 \end{cases}$$

3.3.2. Super twisting sliding mode control

In the existing literature, numerous second-order sliding mode algorithms have been presented. In this research, we utilize the super-twisting control (STSMC) algorithm. Originally conceived in [29] for nonlinear systems featuring a sliding variable with a relative degree of one, this algorithm was subsequently analyzed in [30]. The control objective is to design a suitable control law that allows the system's control output to track the reference trajectory quickly and efficiently.

As we saw previously, we will control the motors to follow the desired trajectory. The sliding surface $S(x,t)$ is defined as (15), (16).

$$S = \beta e + \dot{e} \tag{15}$$

$$\dot{S} = \beta\dot{e} + \ddot{e} \tag{16}$$

Here, $e = \theta - \theta_d$ represents the motor's position tracking error, while β denotes a positive design constant. The corresponding super-twisting control law can be formulated as (17),

$$u = u_{stc} + u_{eq} \tag{17}$$

where

$$u_{stc} = -\lambda|S|^p sign(S) - \int \alpha\, sign(S) \tag{18}$$

The parameters β, λ, and $\alpha$are strictly positive constants, and $p = \frac{1}{2}$. Their values are selected to ensure the stability of the system and the convergence of the tracking error to zero within a finite time. The term u_{eq}denotes the equivalent control, which remains continuous and maintains the system on the sliding surface once this surface has been reached. To keep the system on the sliding manifold, the control u_{eq}must satisfy the algebraic equation (19) to (21).

$$S = \dot{S} = 0 \tag{19}$$

$$\dot{S} = \beta\dot{e} + \ddot{e} = 0 \tag{20}$$

$$\beta\dot{e} + \ddot{e} = \ddot{\theta} - \ddot{\theta_d} + \beta\dot{e} = 0 \tag{21}$$

From (17) and (19) and the equation of the motors (4), (20) becomes (22).

$$u_{eq} = B\left(-\beta\dot{e} + \ddot{\theta_d}\right) + \tau_e \tag{22}$$

The control u became (23).

$$u = B\left(-\beta\dot{e} + \ddot{\theta_d}\right) + \tau_e - \lambda|S|^{\frac{1}{2}} sign(S) - \int \alpha\, sign(S) \tag{23}$$

The stability proof can be found in [30], where geometric methods based on homogeneity are employed to analyze the convergence properties. Moreno and Osorio [32] introduced a quadratic Lyapunov function for the super-twisting controller (STC), which enables the study of finite-time convergence and robustness. In the present work, we consider the quadratic Lyapunov candidate function (24),

$$V = \frac{1}{2} S^T B S \tag{24}$$

where B denotes the inertia matrix of the motors, which is strictly positive definite. Consequently, the Lyapunov function $V$is positive ($V > 0$) and differentiable. According to the Lyapunov stability criterion, if the time derivative $\dot{V}$is strictly negative, the system trajectories will converge to the sliding surface. Thus, we obtain (25) and (26).

$$\dot{V} = \frac{1}{2} \dot{S}^T B S + \frac{1}{2} S^T B \dot{S} + \frac{1}{2} S^T \dot{B} S \tag{25}$$

$$\dot{V} = S^T B \dot{S} + \frac{1}{2} S^T \dot{B} \dot{S} \tag{26}$$

As we said before, B is a constant and strictly positive definite matrix so $\dot{B} = 0$.

$$\dot{V} = S^T B \dot{S} \tag{27}$$

$$\dot{V} = S^T B (\ddot{e} + \beta \dot{e}) \tag{28}$$

$$\dot{V} = S^T B \left(\ddot{\theta} - \ddot{\theta}_d + \beta \dot{e}\right) \tag{29}$$

From the dynamic model (4) and (29), we can write:

$$\dot{V} = S^T B \left(B^{-1}(u - \tau_e) - \ddot{\theta}_d + \beta \dot{e}\right) \tag{30}$$

$$\dot{V} = S^T B \left(B^{-1}\left(B\left(-\beta \dot{e} + \ddot{\theta_d}\right) + \tau_e - \lambda |S|^{\frac{1}{2}} sign(S) - \int \alpha \, sign(S) - \tau_e\right) - \ddot{\theta}_d + \beta \dot{e}\right) \tag{31}$$

$$\dot{V} = -S^T B \lambda |S|^{\frac{1}{2}} sign(S) - S^T B \int \alpha \, sign(S) \tag{32}$$

We note (33).

$$-S^T B \lambda |S|^{\frac{1}{2}} sign(S) < 0 \tag{33}$$

So, we have to demonstrate that $-S^T B \int \alpha \, sign(S) < 0$.

$$sign(S) = \begin{cases} 1 & \text{if} \quad S \geqslant 0 \\ -1 & \text{if} \quad S < 0 \end{cases} \tag{34}$$

$$\int sign\,(S) dt = \begin{cases} t & \text{if} \quad S \geqslant 0 \\ -t & \text{if} \quad S < 0 \end{cases} \tag{35}$$

$$-S \int \alpha \, sign(S) dt = \begin{cases} -\alpha S t & \text{if} \quad S \geqslant 0 \\ \alpha S t & \text{if} \quad S < 0 \end{cases} \tag{36}$$

$$-S \int \alpha \, sign(S) dt = \begin{cases} -\alpha S t < 0 & \text{if} \quad S \geqslant 0 \\ \alpha S t < 0 & \text{if} \quad S < 0 \end{cases} \tag{37}$$

So,

$$-S \int \alpha \, sign(S) < 0 \tag{38}$$

According to (33) and (38), we can conclude that $\dot{V} < 0$. Therefore, based on Lyapunov's theory, System stability under the Super-Twisting control is guaranteed as long as the parameters β, λ, and α remain strictly positive.

3.3.3. Fuzzy logic system

In this part we will use fuzzy logic (FLS) to generate the $sign(S)$ function to increase the robustness of our control against unmodeled noises and to reduce the chattering effect caused by discontinuous control. The FLS will have the sliding surface S and its derivative $\dot{S}$ as inputs and $sign_{fls}(S)$ as output. It is

important to emphasize that the chattering phenomenon occurs when the system states approach the sliding surface $S = 0$. In the proposed solution, the $sign(S)$ function is calculated in the standard way when the system states are far from the sliding surface. Conversely, when the states approach the sliding surface closely, the FLS uses IF-THEN rules to generate the $sign_{fls}(S)$ function and alleviate chattering. Therefore, with this controller, the advantages of using a $sign(S)$ function in STSMC control are preserved, as it continues to bring the system states back toward the sliding surface while effectively eliminating chattering as the system approaches the sliding surface.

The fuzzy input S and $\dot{S}$ are defined as follows: $\{BN, MN, SN, ZE, SP, MP, BP\}$ and the fuzzy output $Sign_f$ is characterized: $\{MN, SN, ZE, SP, MP\}$, where BN= big negative, MN= medium negative, SN= small negative, ZE=Zero, SP= positive small, MP= medium, BP= big positive, we use the triangle membership functions for both fuzzy input and output variables, as shown in Figure 5.

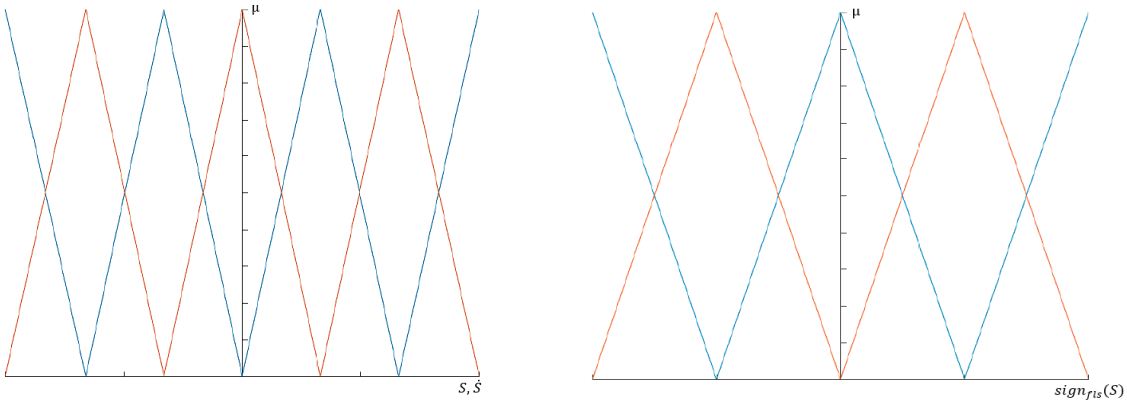

Figure 5. Fuzzy membership function for $S, \dot{S}$ and $sign_{fls}(S)$

We used a base of IF-THEN rules with two entries and a single output (MISO), which is a collection of rules of the following form: R^l: if S is A_S^l and $\dot{S}$ is $A_{\dot{S}}^l$,then $Sign_f$ is B^l or l=1.... N is the number of the rule, S and $\dot{S}$ are the input variables, $Sign_f$ is the output variable and A_S^l, $A_{\dot{S}}^l$ and B^l are the fuzzy sets. The inference system employs the MIN-MAX approach. Additionally, the fuzzy logic technique uses a centroid-type defuzzification mechanism.

4. RESULTS AND DISCUSSION

In this section, our approach is validated through a simulation involving the three joints of the PUMA 560 robot [34]. The task consists in making the robot trace a circular trajectory on the YZ plane while continuously applying a constant desired force of $F_d = 200$ N to the environment. To evaluate the robustness of the proposed method, a disturbance is introduced in the form of an additional mass $m_p = 2\ kg$, applied at time $t = 2\ s$. This mass is not included in the system model and is therefore treated as an unknown disturbance. The stiffness constant of the environment is $K_{env} = 10^4$. The stiffness matrix of the joints is given by $K_e = [\ 7{,}61 * 10^5\ ; 7{,}16 * 10^5; 2{,}16 * 10^5]$.

Figures 6 and 7 represent respectively the joint angle and the motor angle. we also give in Figures 8 and 9 respectively the joint error and the motor error. We observe accurate trajectory tracking of both joint and motor angles. Additionally, the joint angle errors shown in Figure 8 are negligible. We give robot tracking of the desired trajectory in Cartesian space, with its error, respectively in Figures 10 and 11. The error along the X-axis is caused by the end-effector penetrating the environment.

The interaction force generated at the end-effector and its corresponding error with respect to the desired force are presented in Figures 12 and 13, respectively. We will now show in Figure 14 the difference between the motor angle and the joint angle $\alpha = \theta - q$ to visualize the effect of joint flexibility. As we saw previously, joint flexibility generates a difference between the motor angles and the joint angle $\theta \neq q$, and this difference, in our simulation, has a maximum value of $3{,}5 * 10^{-3} rad$. This difference can adversely affect robot performance if it is not taken into account, especially when the robot must apply force to its environment.

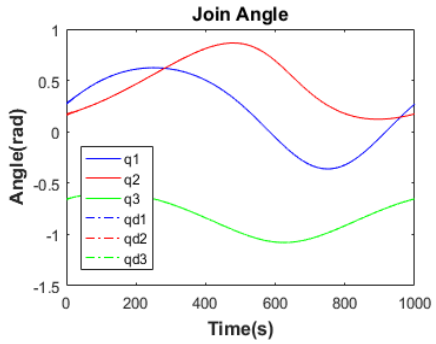

Figure 6. Joint angle

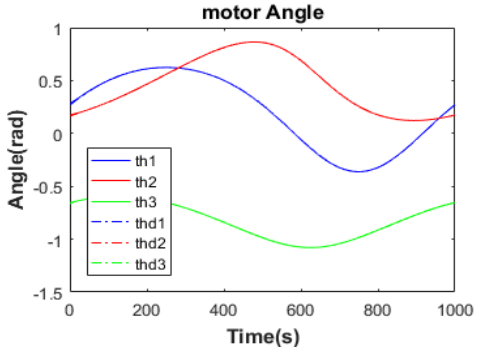

Figure 7. Motor angle

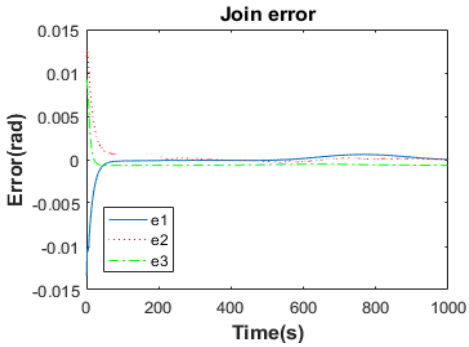

Figure 8. Joint error

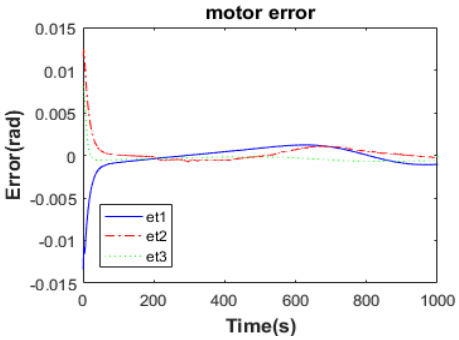

Figure 9. Motor error

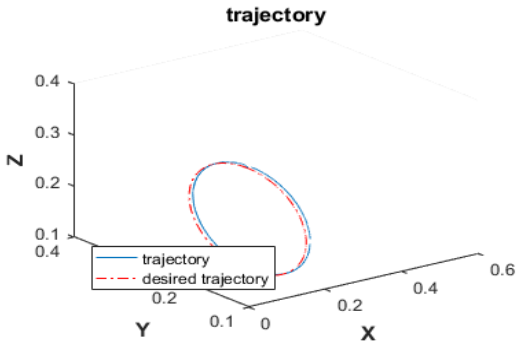

Figure 10. Joint error

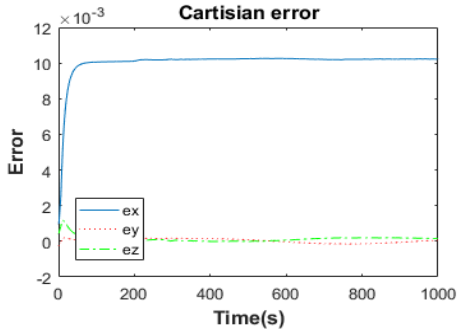

Figure 11. Motor error

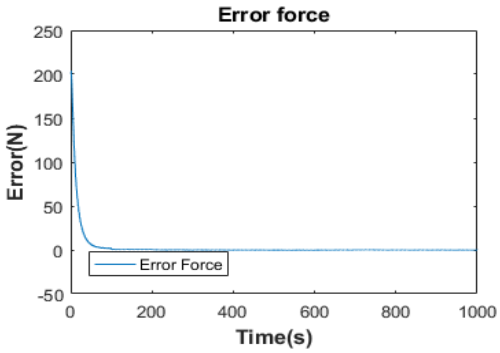

Figure 12. Force

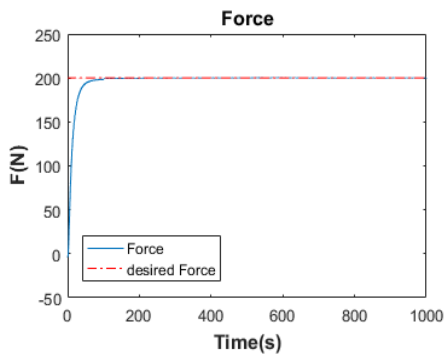

Figure 13. Force error

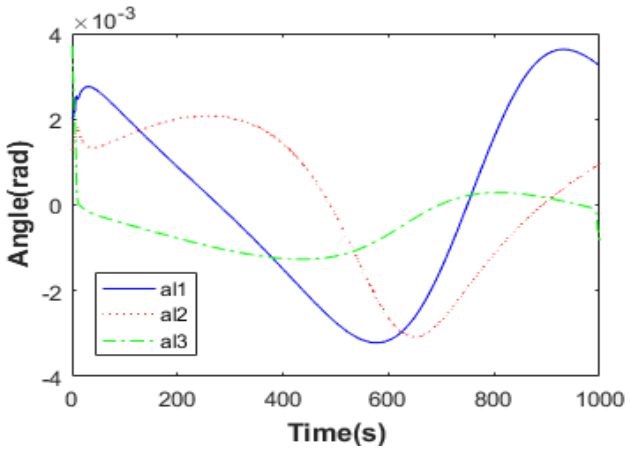

Figure 14. Flexibility effect

5. CONCLUSION

In this paper, a hybrid force-position control strategy for RLFJR has been proposed, integrating fuzzy logic with the FSTSMC approach. The method aims to reduce the negative effects of joint flexibility and improve the tracking accuracy of force and position in constrained environments. Simulation results on the PUMA 560 robot demonstrated that the proposed control strategy enhances robustness to external disturbances and reduces the convergence time of tracking errors compared to conventional methods.

This simulation consisted of making the robot (end-effector) follow a circular trajectory while applying a force to the environment. We presented the simulation results, which we found conclusive, showing the convergence of the error to 0 in a very short time (<1 s) and a substantial decrease of the chattering phenomenon. Future work will focus on experimental validation using a physical robotic platform and extending the approach to multi-contact scenarios or tasks involving dynamic interactions.

FUNDING INFORMATION

No funding was involved.

AUTHOR CONTRIBUTIONS STATEMENT

This journal uses the Contributor Roles Taxonomy (CRediT) to recognize individual author contributions, reduce authorship disputes, and facilitate collaboration.

Name of Author	C	M	So	Va	Fo	I	R	D	O	E	Vi	Su	P	Fu
Rafik Amaini	✓	✓	✓	✓	✓	✓	✓	✓	✓	✓	✓	✓	✓	✓
Farid Ferguene	✓	✓	✓	✓	✓	✓	✓	✓	✓	✓	✓	✓	✓	✓

C : **C**onceptualization
M : **M**ethodology
So : **So**ftware
Va : **Va**lidation
Fo : **Fo**rmal analysis
I : **I**nvestigation
R : **R**esources
D : **D**ata Curation
O : Writing - **O**riginal Draft
E : Writing - Review & **E**diting
Vi : **Vi**sualization
Su : **Su**pervision
P : **P**roject administration
Fu : **Fu**nding acquisition

CONFLICT OF INTEREST STATEMENT

Authors state no conflict of interest.

DATA AVAILABILITY

The data that support the findings of this study are available from the corresponding author, [RA], upon request.

REFERENCES

[1] L. M. Sweet and M. C. Good, "Redefinition of the robot motion-control problem," *IEEE Control Systems Magazine*, vol. 5, no. 3, pp. 18–25, Aug. 1985, doi: 10.1109/MCS.1985.1104955.

[2] M. W. Spong, "On the force control problem for flexible joint manipulators," *IEEE Transactions on Automatic Control*, vol. 34, no. 1, pp. 107–111, Jan. 1989, doi: 10.1109/9.8661.

[3] Y. Liu, X. Luo, and K. Dou, "Control of flexible ankle joint based on singular perturbation theory," in *Proceedings of 2019 IEEE 4th Advanced Information Technology, Electronic and Automation Control Conference, IAEAC 2019*, 2019, pp. 1200–1205, doi: 10.1109/IAEAC47372.2019.8998084.

[4] M. W. Spong, "Modeling and control of elastic joint robots," *Journal of Dynamic Systems, Measurement and Control, Transactions of the ASME*, vol. 109, no. 4, pp. 310–319, Dec. 1987, doi: 10.1115/1.3143860.

[5] K. Khorasani, "Adaptive control of flexible joint robots," in *Proceedings. 1991 IEEE International Conference on Robotics and Automation*, pp. 2127–2134, doi: 10.1109/ROBOT.1991.131942.

[6] R. F. A. Khan, K. Rsetam, Z. Cao, and Z. Man, "Singular perturbation-based adaptive integral sliding mode control for flexible joint robots," *IEEE Transactions on Industrial Electronics*, vol. 70, no. 10, pp. 10516–10525, Oct. 2023, doi: 10.1109/TIE.2022.3222684.

[7] A. De Luca, A. Isidori, and F. Nicolo, "Control of robot arm with elastic joints via nonlinear dynamic feedback," in *Proceedings of the IEEE Conference on Decision and Control*, 1985, pp. 1671–1679, doi: 10.1109/cdc.1985.268819.

[8] K. Khorasani, "Nonlinear feedback control of flexible joint manipulators: a single link case study," *IEEE Transactions on Automatic Control*, vol. 35, no. 10, pp. 1145–1149, Oct. 1990, doi: 10.1109/9.58558.

[9] A. De Luca and P. Lucibello, "A general algorithm for dynamic feedback linearization of robots with elastic joints," in *Proceedings - IEEE International Conference on Robotics and Automation*, 1998, vol. 1, pp. 504–510, doi: 10.1109/ROBOT.1998.677024.

[10] J. Moyron, J. Moreno-Valenzuela, and J. Sandoval, "Nonlinear PID-type control of flexible joint robots by using motor position measurements is globally asymptotically stable," *IEEE Transactions on Automatic Control*, vol. 68, no. 6, pp. 3648–3655, Jun. 2023, doi: 10.1109/TAC.2022.3194043.

[11] M. A. Ahmad, H. Ishak, A. N. K. Nasir, and N. A. Ghani, "Data-based PID control of flexible joint robot using adaptive safe experimentation dynamics algorithm," *Bulletin of Electrical Engineering and Informatics*, vol. 10, no. 1, pp. 79–85, Feb. 2021, doi: 10.11591/eei.v10i1.2472.

[12] Z. Wenhui *et al.*, "Improved sliding mode variable structure control of robot manipulators with flexible joints based on singular perturbation," in *Proceedings - 2023 International Conference on Telecommunications, Electronics and Informatics, ICTEI 2023*, 2023, pp. 288–291, doi: 10.1109/ICTEI60496.2023.00084.

[13] Y. Zhang, L. Wang, L. Liu, and Y. Guo, "Sliding mode control for flexible joint space robot via nonlinear integration," in *Proceedings of the 4th Conference on Fully Actuated System Theory and Applications, FASTA 2025*, 2025, pp. 2320–2324, doi: 10.1109/FASTA65681.2025.11138780.

[14] J. De Leon-Morales and J. G. Alvarez-Leal, "Comparative study of speed and position control of a flexible joint robot manipulator," in *IEEE International Conference on Intelligent Robots and Systems*, 1998, vol. 1, pp. 679–684, doi: 10.1109/iros.1998.724697.

[15] L. Zouari, H. Abid, and M. Abid, "Comparative study between PI and sliding mode controllers for flexible joint manipulator driving by Brushless DC motor," in *14th International Conference on Sciences and Techniques of Automatic Control and Computer Engineering, STA 2013*, 2013, pp. 294–299, doi: 10.1109/STA.2013.6783146.

[16] M. Jankovic, "Observer-based control for elastic joint robots," *IEEE Transactions on Robotics and Automation*, vol. 11, no. 4, pp. 618–623, Aug. 1995, doi: 10.1109/70.406947.

[17] J. Lee, T. J. Ha, J. S. Yeon, S. Lee, and J. H. Park, "Robust nonlinear observer for flexible joint robot manipulators with only motor position measurement," in *ICCAS 2007 - International Conference on Control, Automation and Systems*, 2007, pp. 56–61, doi: 10.1109/ICCAS.2007.4406879.

[18] H. Ma, H. Ren, Q. Zhou, H. Li, and Z. Wang, "Observer-based neural control of N-link flexible-joint robots," *IEEE Transactions on Neural Networks and Learning Systems*, vol. 35, no. 4, pp. 5295–5305, Apr. 2024, doi: 10.1109/TNNLS.2022.3203074.

[19] L. Huang, S. S. Ge, and T. H. Lee, "Position/force control of uncertain constrained flexible joint robots," *Mechatronics*, vol. 16, no. 2, pp. 111–120, Mar. 2006, doi: 10.1016/j.mechatronics.2005.10.002.

[20] T. Shi, Y. Pan, and C. Wen, "Modern compliant robot control: exploring benefits from singular perturbation synthesis," *IEEE Transactions on Industrial Electronics*, vol. 72, no. 3, pp. 2758–2768, Mar. 2025, doi: 10.1109/TIE.2024.3426053.

[21] Y. R. Hu and G. Vukovich, "Position and force control of flexible joint robots during constrained motion tasks," *Mechanism and Machine Theory*, vol. 36, no. 7, pp. 853–871, Jul. 2001, doi: 10.1016/S0094-114X(01)00021-0.

[22] K. P. Jankowski and H. A. ElMaraghy, "Nonlinear decoupling for position and force control of constrained robots with flexible joints," in *Proceedings - IEEE International Conference on Robotics and Automation*, 1991, vol. 2, pp. 1226–1231, doi: 10.1109/robot.1991.131779.

[23] S. Ahmad, "Constrained motion (force/position) control of flexible joint robots," in *Proceedings of the IEEE Conference on Decision and Control*, 1991, vol. 2, pp. 1397–1402, doi: 10.1109/cdc.1991.261629.

[24] S. Ding, J. Peng, Y. Hou, and X. Lei, "Neural network-based hybrid position/force tracking control for flexible joint robot," in *SYSCON 2020 - 14th Annual IEEE International Systems Conference, Proceedings*, 2020, pp. 1–6, doi: 10.1109/SysCon47679.2020.9275663.

[25] H. Yin, S. Li, and H. Wang, "Sliding mode position/force control for motion synchronization of a flexible-joint manipulator system with time delay," in *Chinese Control Conference, CCC*, 2016, vol. 2016-August, pp. 6195–6200, doi: 10.1109/ChiCC.2016.7554329.

[26] M. Farooq and D. B. Wang, "Hybrid force/position control scheme for flexible joint robot with friction between and the end-effector and the environment," *International Journal of Engineering Science*, vol. 46, no. 12, pp. 1266–1278, Dec. 2008, doi: 10.1016/j.ijengsci.2008.06.010.

[27] A. Levant, "Quasi-continuous high-order sliding-mode controllers," *IEEE Transactions on Automatic Control*, vol. 50, no. 11, pp. 1812–1816, Nov. 2005, doi: 10.1109/TAC.2005.858646.

[28] A. Ferrara and G. P. Incremona, "Robust motion control of a robot manipulator via Integral Suboptimal Second Order Sliding modes," in *Proceedings of the IEEE Conference on Decision and Control*, 2013, pp. 1107–1112, doi: 10.1109/CDC.2013.6760030.

[29] S. Kochetkov, S. A. Krasnova, and V. A. Utkin, "The new second-order sliding mode control algorithm," *Mathematics*, vol. 10, no. 13, p. 2214, 2022, doi: 10.3390/math10132214.

[30] A. Levant, "Sliding order and sliding accuracy in sliding mode control," *International Journal of Control*, vol. 58, no. 6, pp. 1247–1263, Dec. 1993, doi: 10.1080/00207179308923053.
[31] J. A. Moreno and M. Osorio, "Strict Lyapunov functions for the super-twisting algorithm," *IEEE Transactions on Automatic Control*, vol. 57, no. 4, pp. 1035–1040, Apr. 2012, doi: 10.1109/TAC.2012.2186179.
[32] J. A. Moreno and M. Osorio, "A Lyapunov approach to second-order sliding mode controllers and observers," in *Proceedings of the IEEE Conference on Decision and Control*, 2008, pp. 2856–2861, doi: 10.1109/CDC.2008.4739356.
[33] J. De Schutter and H. Van Brussel, "Compliant robot motion II: a control approach based on external control loops," *The International Journal of Robotics Research*, vol. 7, no. 4, pp. 18–33, Aug. 1988, doi: 10.1177/027836498800700402.
[34] B. Armstrong, O. Khatib, and J. Burdick, "Explicit dynamic model and inertial parameters of the PUMA 560 arm," in *Proceedings of the IEEE International Conference on Robotics and Automation*, 1986, pp. 510–518, doi: 10.1109/robot.1986.1087644.

BIOGRAPHIES OF AUTHORS

Rafik Amaini received his master's degree in Automation from the University of Science and Technology Houari Boumediene (USTHB), Algiers, Algeria, in 2014. He is currently a Ph.D. candidate in the LRPE Laboratory at USTHB. His main research interests include industrial robotics with flexible joints, nonlinear control, force and position control, and hybrid intelligent control methods. He is particularly focused on the development of robust and adaptive control strategies for constrained environments. He is also passionate about embedded systems and real-time implementation of advanced controllers. He can be contacted at rafik.amaini@gmail.com.

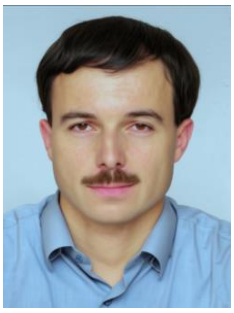

Farid Ferguene received his engineer degree from the University of the Sciences and Technology, Houari Boumediene (USTHB), Algeria, in 1993. In 1994 he joined the LRPE laboratory of the same university, where he received his M.Sc. and Ph.D. degrees in 1997 and 2008, respectively. All his degrees are in electronic engineering. He is a USTHB university professor and team leader at LRPE Laboratory. His research interests include advanced systems control and robotics. He can be contacted at fferguene@yahoo.fr.